International Journal of GEOMATE, Oct., 2024 Vol.27, Issue 122, pp.28-35
ISSN: 2186-2982 (P), 2186-2990 (O), Japan, DOI: https://doi.org/10.21660/2024.122.4484
Geotechnique, Construction Materials and Environment

GRAPHICAL REPRESENTATION OF UNIAXIAL TENSILE TEST THROUGH DIGITAL IMAGE CORRELATION

Cintantya Budi Casita[1], *Data Iranata[1], Budi Suswanto[1] and Masahide Matsumura[2]

[1]Department of Civil Engineering, Institut Teknologi Sepuluh Nopember, Indonesia;
[2]Department of Civil Engineering, Kumamoto University, Japan

*Corresponding Author, Received: 03 Aug. 2024, Revised: 13 May 2024, Accepted: 28 July 2024

ABSTRACT: Digital Image Correlation (DIC) is a non-contact measurement method that identifies surface changes on a specimen by analyzing a sequence of photographs taken before, during, and after the loading process. DIC determines contour deformation, strain, and stress values by examining variations in the speckled pattern created by the random addition of black dots. In this research, DIC was used to visualize the graphical presentation of a uniaxial tensile test. To obtain stress and strain values, the study employed two methods: the conventional experimental uniaxial tensile test and the DIC method. Tensile steel specimens with five different thicknesses, ranging from 6 mm to 16 mm, were fabricated and tested. The specimens were cut at a 15-degree angle from the rolling direction from the same plate sheet for each thickness. It was discovered that the orientation of the applied forces can affect the changes in Young's modulus values, which are higher when the load is applied parallel to the direction rather than perpendicular to it. The open-source image correlation software package Ncorr, integrated with MATLAB, was used for DIC analysis. The results showed that both methods provided close values for tensile strength and Young's modulus. The DIC method produced slightly lower values than the conventional technique but was still considered accurate for predicting tensile properties. The DIC models also demonstrated good agreement with the experimental findings, suggesting its suitability as a straightforward evaluation method for predicting tensile properties.

Keywords: Tensile test, Tensile properties, Digital image correlation, Ncorr, Strain fields

1. INTRODUCTION

Digital image correlation (DIC) is a non-contact optical measurement method that provides full-field deformation and strain fields at various scales. It quantifies surface changes on a specimen using visual measurement techniques [1]. DIC determines the deformation of the specimen by analyzing a sequence of photographs taken before, during, and after applying a load [1–3]. The analysis relies on a speckled pattern created by randomly applying black dots (typically in a black-and-white combination). The changes in this pattern due to loading are tracked through a series of photographs captured with a digital camera over time [4]. DIC enables the evaluation of strain, stress, and displacement across an object's entire surface without using instruments such as strain gauges, transducers, or linear variable differential transformers. Since its introduction in the 1980s, this technique has been applied to various fields beyond engineering. [5,6]. In recent years, it has been increasingly used to measure stress-strain deformation behavior [7–9], residual stress [10–12], lifespan [13], integrity, and durability [14], and cracks [15,16]. For example, the DIC technique has been applied to bone specimens to understand the surface strain under compressive loading [17]. Other applications have revealed the response of residual interfacial stress, which approximates the uniaxial stress state of thermal barrier coatings [18].

Numerous studies have examined the tensile properties of various materials using the DIC technique. For example, Tambusay et al. [19] DIC was applied to determine crack propagation in engineered cementitious composite concrete under a four-point bending test. Cerbu et al. [21] Used DIC to evaluate Poisson's ratio for composite materials and an aluminum alloy under tensile testing. This technique has also been advanced to predict the uniaxial stress-strain response of numerous stainless-steel specimens, highlighting its versatility and potential for gauging full-field deformation under thermo-mechanical loading. Chevalier et al. [22] Explored the multiaxial characteristics of rubber-like materials using DIC, discerning heterogeneous strain fields under biaxial loading conditions. This research underscores the DIC method's applicability across diverse material types and loading scenarios, offering valuable insights into their mechanical responses. In addition, Oh et al. [23] and Roudsari et al. [24] conducted studies to clarify the DIC process, while Brillaud et al. [25] and Harilal et al. [26] used a sequent to capture proper images using a low-cost approach.

While previous studies have explored the tensile properties of various materials, limited research has compared and analyzed the accuracy of different measurement techniques. This paper is part of extensive research aimed at identifying the behavior of steel sections with varying thicknesses of steel

segments, using a variety of stiffeners as support. The specimens were obtained from the same plate sheet for each thickness and cut at a 15-degree angle from the rolling direction, ensuring consistent conditions across varying thicknesses. The purpose of this uniaxial tension test was to examine the material's plastic anisotropy in different directions. The study aimed to comprehensively understand the tensile properties using two distinct methods: experimental and DIC techniques.

The study focused on steel materials with a thickness of 6 to 16 mm, examining parameters such as maximum stress and Young's modulus. The stress–strain response of the specimens tested was captured, and the effect of thickness on these parameters was analyzed based on the test results. Furthermore, a monitoring system based on DIC was integrated to determine the failure mechanisms of the specimens. Consequently, positive correlations were expected among the research analysis outcomes, including experimental testing and monitoring systems.

2. RESEARCH SIGNIFICANCE

The study aimed to examine the fundamental parameters and composition of steel properties by evaluating the material's behavior. Although prior research has investigated the characteristics of various materials, few studies have assessed the precision of measurement methodologies using specimens of different thicknesses and the plastic anisotropy behaviors of materials in multiple directions. Critical insights into the failure mechanisms can be obtained by monitoring specimens and employing intelligent data analytics for evaluations. The findings of this research will contribute to the development of an advanced yet straightforward DIC-based monitoring system, thereby facilitating further investigations.

3. EXPERIMENTAL PROGRAM

3.1 Fabrication Process and Preparation

A series of steel materials, classified as grade 41, were used to study tensile properties and served as stiffeners on the beam–column joint segment. The dimensions of the tensile specimen are illustrated in Fig. 1 in accordance with ASTM E8/E8M [27]. Specimens with five different thicknesses were prepared for testing under the uniaxial tensile test. The steel for each specimen was cut using a grinding cutting machine, with different cutting edges employed for various thicknesses to achieve consistent dimensions. A paper plot was also added to the specimen before the cutting process to ensure uniform dimensions.

After obtaining the dimensions, the specimen was painted using white Pylox spray paint. The spray was applied lightly to create a layered pattern before adding the random black dots. These dots are crucial for the DIC technique, which requires dividing the object into small subsets to obtain the full deformation field of the specimen. The subsets are created from the black dots. To ensure the dots or speckle patterns were random, two sizes of permanent markers were used.

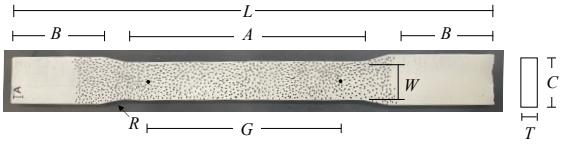

Fig.1. Tensile test specimen – ASTM E8/E8M

Table 1. Detail dimension of tensile test specimen

Dimension	mm
Gauge length, G	200 ± 0.2
Width, W	40 ± 2.0
Radius of fillet, R	25
Overall length, L	450
Min. length of reduced section, A	225
Min. length of grip section, B	75
Width of grip section, C	50
Thickness of material, T	
Specimen I	6
Specimen II	8
Specimen III	10
Specimen IV	12
Specimen V	16

To ensure that each subset has its own distinctive characteristics, it was necessary to implement a speckle pattern with identifiable, irregular features throughout its region [28]. Key parameters include speckle dimension [29], pattern contrast [30], edge sharpness of the speckle [31], and speckle density [32]. For a pattern to be identified as non-repeating and isometric, there must be sufficient contrast between its light and dark portions to detect every distinctive feature. The contrast of the pattern is influenced by factors such as the intensity of the lighting source, the size of the lens aperture, the exposure time of the camera, and the type of paint applied for the speckle [33,34].

To identify a pattern as non-repeating and isometric, there must be sufficient contrast between the pattern's light and dark portions for every distinctive feature to be detected. This contrast is influenced by factors such as the intensity of the lighting source, the size of the lens aperture, the exposure time of the camera, and the type of paint applied for the dots [33].

3.2 Uniaxial Tensile Test

The tensile test was performed using a universal

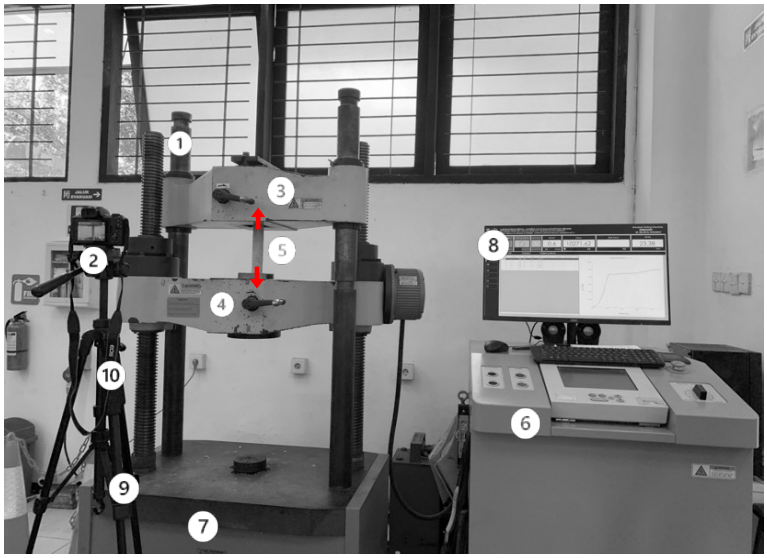

Information:
1. Screw support
2. Low-cost digital image correlation system using digital camera
3. Adjustable upper crosshead
4. Adjustable lower crosshead
5. Test Specimen
6. Electronic control panel
7. Universal Testing Machine 1000 kN
8. Monitor to reflect displacement
9. Tripod
10. Extended cable

Detail of Specimen No. 5 Speckle Pattern for Interpreting Image Correlation Technique

Fig.2 Illustrated specimen under Universal Testing Machine Shimadzu UH-500

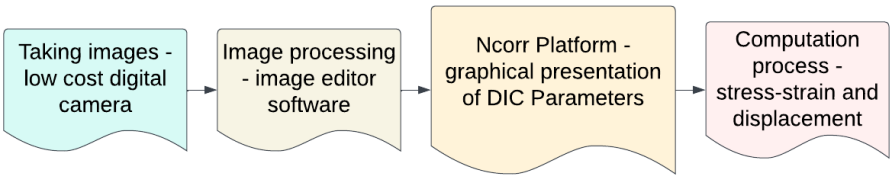

Fig.3 The DIC technique step by step analysis

testing machine (Shimadzu UH-500) with a maximum load of capacity 500 kN and a displacement rate of 0.6 mm/min, in accordance with ASTM 638. The specimen was gripped on both sides, and tensile strain was measured in the central part of the specimen. A displacement transducer was also mounted at the back of the central neck of the specimen (see Fig. 2). The stress–strain data were obtained during the test using Shimadzu software developed by the Laboratory of Concrete, Advanced Materials and Computational Mechanics ITS. The tensile test was recorded using a Canon M50 Mark II digital camera to support the DIC, capturing a series of images. Fig. 2 illustrates the tensile test experimental setup using the low-cost DIC technique.

To identify several parameters, basic engineering property equations were inputted into the calculations, such as tensile stress–strain (σ–ε) and Young's modulus (E). These equations demonstrate the stiffness of steel materials under the stress–strain relationship in the linear elastic deformation stage, which follows Hooke's law. The equation is shown as follows:

$$\sigma = \frac{P}{A_0} \tag{1}$$

$$\varepsilon = \frac{\Delta L}{L_0} = \frac{L_f - L_0}{L_0} \tag{2}$$

$$E = \frac{\sigma}{\varepsilon} \tag{3}$$

The stress value, σ, is determined by dividing the axial load during the tensile test, P, by the cross-sectional area of the specimen, A_0, as represented by Equation (1). The tensile strain, ε, is calculated by dividing the change in length, ΔL, by the original length, L_0, as expressed in Equation (2).

3.3 Digital Image Correlation (DIC) Technique

The step-by-step DIC technique is illustrated in Fig. 3, including image capture with a low-cost digital camera, image processing, the Ncorr platform, and the computation process. The images were captured at a resolution of 4608×3072 pixels using a Canon M50 Mark II digital camera. The camera position needed to be steady and properly aligned to provide clear, non-blurry images. Due to the fixed position of the UTM, the camera was placed 500 mm away on a steady tripod. The first image was captured as the control before loading, with subsequent images taken at loading increments until the specimen failed. The total duration of the tensile test and the expected number of images defined the capture intervals. During image processing, the acquired digital images were automatically enhanced using image editing software to improve quality and clarity. This step was

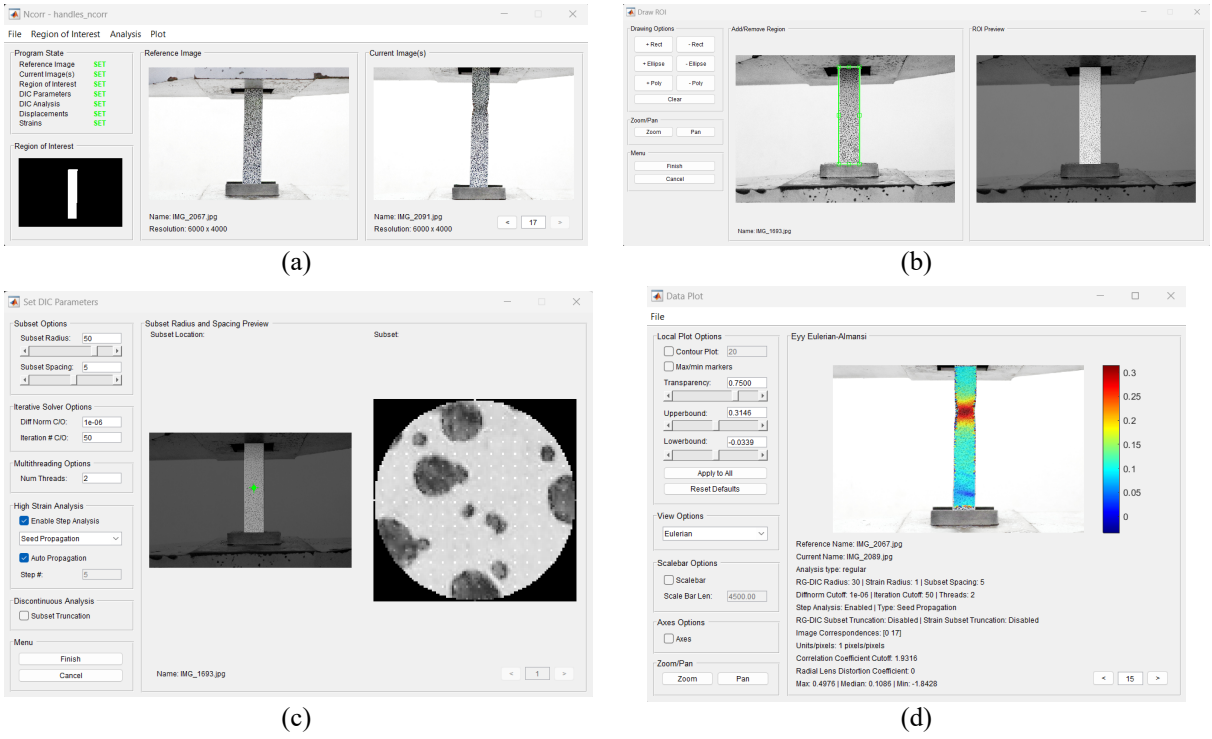

Fig.4. (a) Ncorr main interface, (b) Region of Interest of tensile specimen, (c) Image reference partitioned into small subset, (d) Identified strain response

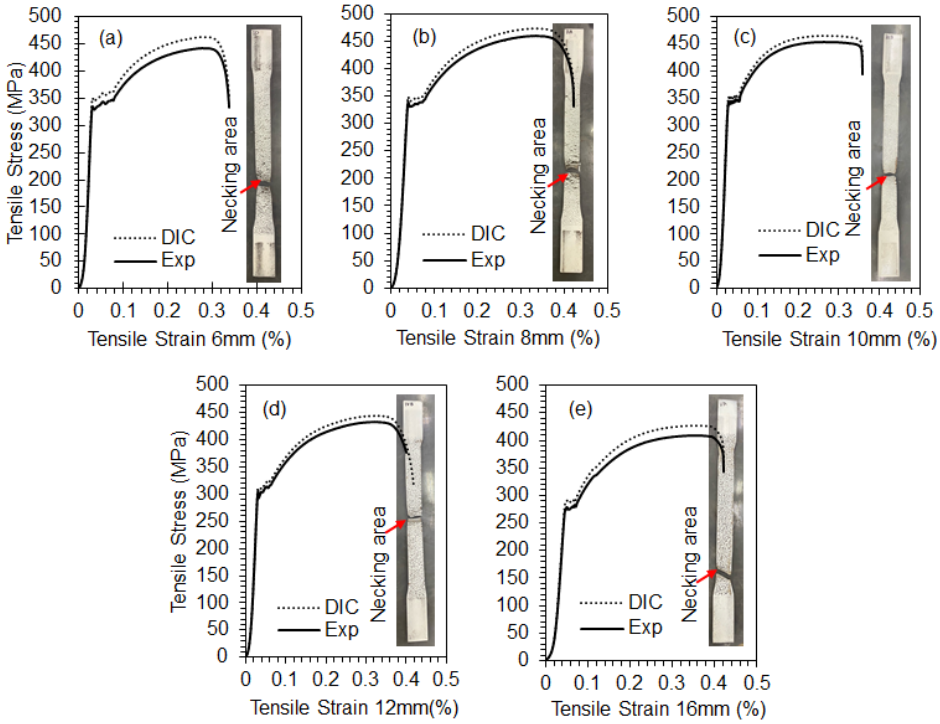

Fig.5. Graph of tensile stress vs. tensile strain under different thickness

performed to ensure sufficient contrast between the light and dark parts of the pattern, allowing the DIC algorithm to accurately identify each distinct component.

The next step involves using the Ncorr platform, open-source software that graphically analyzes the images and converts them into stress–strain and displacement data. In this study, Ncorr 1.1.2 and MATLAB R2021 were used. During this stage, the graphical presentation of DIC parameters is designed

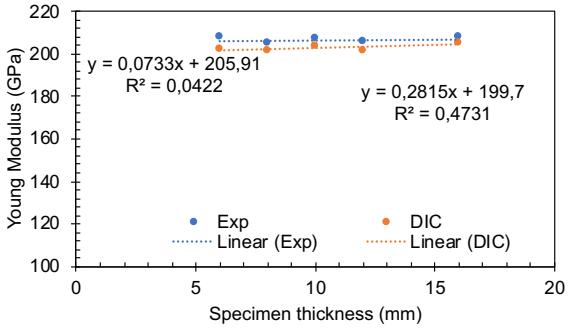

Fig. 6. Young modulus result under different thickness

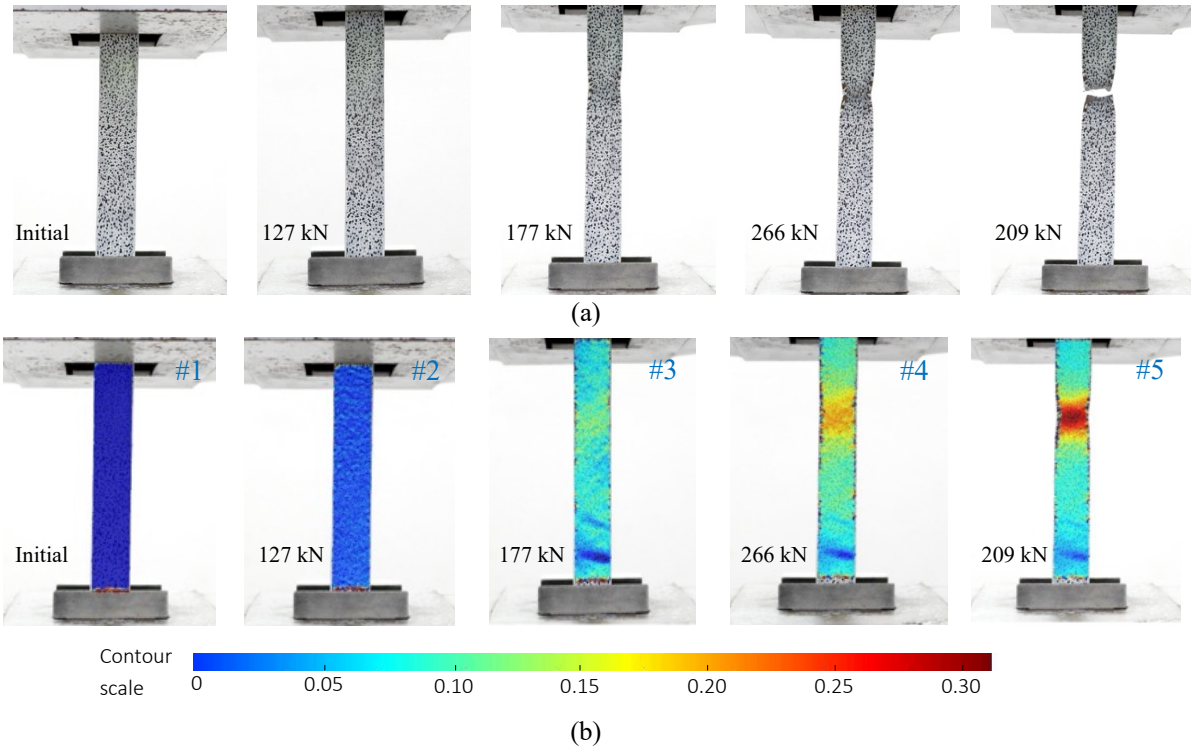

Fig. 7. The example of (a) observed crack pattern, (b) DIC modeling analysis in each loading phase – 8 mm thickness

to meet specific conditions. The platform uses an image registration technique to map both local and global displacements, allowing for the derivation of strains.

Fig. 4(a) presents the Ncorr main user interface, illustrating its primary layout. To initiate the DIC analysis, users must first upload a reference image of the specimen before loading, which will then be displayed in the left-hand side window of the main terminal. Subsequently, a sequence of images captured during testing should be uploaded. Each collection of small subsets is governed by two parameters: subset radius (r) and subset spacing (s). When r equals half of s, the subsets take the shape of contiguous circles with a radius of r. Within Ncorr, deformation within each subset is assumed to be uniform.

The displacement field of a subset is initially determined by evaluating a cost function, mainly through normalized cross-correlation, providing an initial estimation of the displacement. To enhance the accuracy of this estimation, the inverse compositional Gauss–Newton method is applied. This method iteratively adjusts the displacement field by minimizing the difference between the observed subset and the reference subset, resulting in a refined displacement field [35]. This iterative refinement process ensures a more precise alignment between corresponding subsets in the reference and target images, leading to improved accuracy in the overall deformation analysis. Afterward, users must define the region of interest (ROI), as illustrated in the right-hand side window in Fig. 4(b), delineating the area for the DIC analysis.

To capture the complete deformation field, the object's image must be partitioned into small subsets (see Fig. 4(c) for illustration). Each subset requires a distinct pattern to enable the algorithm to differentiate accurately between them, facilitating the matching of target and reference subset blocks.

Using the center-point locations of subsets in both the reference and target images, a local displacement vector is generated, and deformation within each subset is calculated. This iterative process is applied to all subset blocks across the entire surface of the object, resulting in a comprehensive displacement map. From this map, strains can be derived [17].

In Ncorr, digital images are depicted as a collection of small subsets governed by two parameters: subset radius (r) and subset spacing (s). When r equals half of s, the subsets take the shape of contiguous circles with a radius of r. Within Ncorr, deformation within each subset is assumed to be uniform. The displacement field of a subset is initially determined by evaluating a cost function, mainly through normalized cross-correlation, providing an initial estimation of the displacement.

Subsequently, to enhance the accuracy of this estimation, the inverse compositional Gauss-Newton method is applied. This method iteratively adjusts the displacement field by minimizing the difference between the observed subset and the reference subset, resulting in a refined displacement field [35]. This iterative refinement process ensures a more precise alignment between corresponding subsets in the reference and target images, leading to improved accuracy in the overall deformation analysis. In addition to these functionalities, Ncorr can execute multi-thread computations and manage tasks involving large deformation, rigid-body deformation, and strong discontinuities. Fig. 4(d) provides an example of the identified strain response obtained from a DIC analysis.

4. RESULTS AND DISCUSSION

Tensile tests with different steel thicknesses were conducted using uniaxial tensile tests and the DIC technique. The results are discussed below.

4.1 Tensile Test Result

Fig. 5 shows the tensile test results for different thicknesses, along with failure illustrations, compared to the DIC analysis. Each specimen was observed to exhibit a similar trend. The maximum tensile stress for the experimental test was 460 MPa, while the DIC technique measured it at 473 MPa for the 8 mm thick specimen. The stress vs. strain curve for the DIC technique showed a slightly higher trend compared to the conventional technique during the elastic phase.

For the 10 mm specimen, the maximum stress decreased to 454 MPa, with further decreases observed for the 12 mm and 16 mm specimens. The DIC technique confirmed the experimental test results, showing similar trends. This decrease in tensile strength may be attributed to the higher cross-sectional area, which significantly affects tensile strength. The tightness of the grip during the test also plays a crucial role in determining tensile strength, as a secure grip is essential for accurate measurements.

In such cases, increasing the thickness of the specimen may not proportionately enhance the tensile strength. Factors such as material ductility, flaws, and structural design significantly influence the overall strength. Finding the right balance between thickness and these other considerations is crucial to achieving optimal strength and performance.

Young's modulus was analyzed and compared to better comprehend the stiffness in this study. The results of Young's modulus for each material thickness are summarized in Fig. 6. All testing methods yielded similar values for Young's modulus. It was determined that the orientation of applied forces can impact the variations in Young's modulus values, which exhibit larger values when the load is applied in parallel with the direction, as opposed to perpendicular to it. The Young's modulus, E, for steel is supposed to be 210 GPa, as shown by comparisons to theoretical reference. Consequently, the average value of Young's modulus of the steel under experimental and DIC method was determined to be 206 ± 2 GPa and 201 ± 2 GPa, respectively, which deviates from the reference value of the Young's modulus by 1.58% and 3.51%. Regarding the testing technique, the DIC method yielded slightly lower values than the experimental results. Overall, it was concluded that the DIC method is adequate for evaluating the tensile properties under tensile loading conditions.

4.2 DIC Techniques Results

The contour plot image was generated using the DIC Ncorr within MATLAB software, applied under tensile loading conditions. Fig. 7(b) shows the contour plot of measured strain during tensile loading, illustrating parameters such as analysis type, subset criteria, and step analysis. Color coding represents the stress–strain criteria. The same figure also displays the contour plot of strain values for the 8 mm thick tensile steel specimen, highlighting the trend in strain development. Both the experimental and DIC methods detected and observed the necking area, as shown in Fig. 7(a) and Fig. 7(b). In addition, the maximum strain value (shown in red) was 0.43, while the minimum strain value (shown in blue) was approximately 0.

5. CONCLUSIONS

The DIC technique has gained increasing attention for its ability to map strain and displacement effectively. In this study, tensile steel specimens of varying thicknesses were used to explore their tensile properties using two methods: conventional uniaxial testing and DIC. The conventional technique generated an average Young's modulus measurement of 206 ± 2 GPa, while the DIC method obtained an average value of 201 ± 2 GPa. These values deviate from the theoretical reference value of the elastic modulus by 11.58% and 3.51%, respectively. From a methodological standpoint, the DIC technique yielded results comparable to those of the conventional test, with slightly higher values. Furthermore, it demonstrated reasonable agreement with the experimental findings, indicating its suitability as a straightforward method for predicting tensile properties.

6. ACKNOWLEDGMENTS

The authors would like to acknowledge the support of the Laboratory of Structure at Sepuluh Nopember Institute of Technology. They also wish to express their gratitude for the financial support provided by the Sepuluh Nopember Institute of Technology under research fund contract number 1716/PKS/ITS/2023, as well as the support from the Ministry of Finance of the Republic of Indonesia through the Indonesia Endowment Fund for Education Agency, with contract number 202207210110707.

7. REFERENCES

[1] Dong Y.L., and Pan B., A Review of Speckle Pattern Fabrication and Assessment for Digital Image Correlation. Experimental Mechanics, Vol. 57, Issue 8, 2017, pp. 1161–1181.

[2] Zhang X., and Ricles J.M., Seismic Behavior of Reduced Beam Section Moment Connections to Deep Columns. Journal of Structural Engineering, Vol. 132, Issue 3, 2006, pp. 358–367.

[3] Baqersad J., Carr J., Lundstrom T., Niezrecki C., Avitabile P., and Slattery M., Dynamic Characteristics of A Wind Turbine Blade using 3D Digital Image Correlation. Health Monitoring of Structural and Biological Systems 2012, Vol. 8348, Issue 74, 2012, pp. 711–719.

[4] Brillaud J., and Lagattu F., Limits and Possibilities of Laser Speckle and White-Light Image-Correlation Methods: Theory and Experiments. Applied Optics, Vol. 41, Issue 31, 2002, pp. 6603–6613.

[5] Fanaie N., and Moghadam H.S., Experimental study of rigid connection of drilled beam to CFT column with external stiffeners. Journal of Constructional Steel Research, Vol. 153, 2019, pp. 209–221.

[6] Lim S.H., Zeng K.Y., and He C.B., Morphology, tensile and fracture characteristics of epoxy-alumina nanocomposites. Materials Science and Engineering: A, Vol. 527, Issue 21–22, 2010, pp. 5670–5676.

[7] Jarrett S.R., Thai T.Q., Rowley L.J., Craig W.D., and Berke R.B., The Effect of Bit Depth on High-Temperature Digital Image Correlation Measurements. Journal of Sensors, Vol. 2022, Issue 1, 2022, pp. 6554128.

[8] Arola A.M., Kaijalainen A., Kesti V., Pokka A.P., and Larkiola J., Digital image correlation and optical strain measuring in bendability assessment of ultra-high strength structural steels, Conference proceedings, In: Procedia Manufacturing on SHEMET, Elsevier B.V., Vol. 29, 2019, pp. 398–405.

[9] Chai J., Liu Y., Ouyang Y.B., Zhang D., and Du W., Application of Digital Image Correlation Technique for the Damage Characteristic of Rock-like Specimens under Uniaxial Compression. Advances in Civil Engineering, Vol. 2020, Issue 1, 2020, pp. 8857495.

[10] Lord J.D., Penn D., and Whitehead P., The application of digital image correlation for measuring residual stress by incremental hole drilling. In: Applied Mechanics and Materials. Trans Tech Publications Ltd, Vol. 13-14, Issue 6, 2008, pp. 65–73.

[11] Chien C.-H., Su T.-H., Wang C.-T., Chen B.-S., and Su -H, Using Digital Image Correlation Method for Measuring Residual Stress in the Nickel Coating of the Specimen, Vol. 40, Issue 4, 2016, pp. 1341-1348.

[12] Boruah D., Dewagtere N., Ahmad B., Nunes R., Tacq J., Zhang X., Guo H., Verlinde W., and De Waele W., Digital Image Correlation for Measuring Full-Field Residual Stresses in Wire and Arc Additive Manufactured Components. Materials, Vol. 16, Issue 4, 2023, pp. 1702.

[13] Zhang X., Ricles J.M., Lu L., and Fisher J.W., Analytical and Experimental Studies on Seismic Behavior of Deep Column-to-Beam Welded Reduced Beam Section Moment Connections, Conference proceedings, in 13th World Conference on Earthquake Engineering, Vol. 1, Issue 113, 2004, pp. 1599.

[14] Schijve J., Fatigue of Structures and Materials, A book Springer Dordrecht Publisher, Vol. 25, 2003, pp. 1–623.

[15] Christensen C.O., Schmidt J.W., Halding P.S., Kapoor M., and Goltermann P., Digital image correlation for evaluation of cracks in reinforced

concrete bridge slabs Infrastructures, Vol. 6, Issue 7, 2021, pp. 99.
[16] Irmawan M., Piscesa B., Suprobo P., and Alrasyid H., Application of Digital Image Correlation to Capture The Crack Mouth Opening Displacement Of The Notched Steel Fiber Reinforced Concrete (SFRC) Beam, Vol. 37, Issue 2, 2022. pp. 94-100.
[17] Melinda A.P., Yoresta F.S., Higuchi S., Yamazaki Y., and Matsumoto Y., Investigation of the accuracy of Digital Image Correlation (DIC) in measuring full-field strain for timber materials, Conference proceedings, In: E3S Web of Conferences. EDP Sciences, Vol. 464, 2023, pp. 09002.
[18] Quanjin M., Rejab M.R.M., Halim Q., Merzuki M.N.M., and Darus M.A.H., Experimental investigation of the tensile test using digital image correlation (DIC) method Conference proceedings, In: Materials Today: Proceedings. Elsevier Ltd, Vol. 27, Issue 2, 2020, pp. 757–763.
[19] Tambusay A., Suryanto B., and Suprobo P., Digital Image Correlation for Cement-based Materials and Structural Concrete Testing. Civil Engineering Dimension, Vol. 22, Issue 1, 2020, pp. 6–12.
[20] Cerbu C., Xu D., Wang H., and Roşca I.C., The use of Digital Image Correlation in determining the mechanical properties of materials, Conference proceedings, In: IOP Conference Series: Materials Science and Engineering. Institute of Physics Publishing, Vol. 399, 2018, pp. 012007.
[21] Chevalier L., Calloch S., Hild F., and Marco Y., Digital image correlation used to analyze the multiaxial behavior of rubber-like materials. Vol. 20, Issue 2, 2001, pp. 169–187.
[22] Oh K., Lee K., Chen L., Hong S. Bin, and Yang Y., Seismic performance evaluation of weak axis column-tree moment connections with reduced beam section. Journal of Constructional Steel Research, Vol. 105, Issue 8, 2015, pp. 28–38.
[23] Roudsari M.T., Abdollahi F., Salimi H., Azizi S., and Khosravi A.R., The Effect of Stiffener on Behavior of Reduced Beam Section Connections in Steel Moment-Resisting Frames. International Journal of Steel Structures, Vol. 15, Issue 4, 2015, pp. 827–834.
[24] Brillaud J., and Lagattu F., Limits and Possibilities of Laser Speckle and White-Light Image-Correlation Methods: Theory and Experiments, Journal of Applied Optics, Vol. 41, Issue 31, 2002, pp. 6603-6613.
[25] Harilal R., and Ramji M., Adaptation of Open Source 2D DIC Software Ncorr for Solid Mechanics Applications, Conference proceedings, in 9th International Symposium on Advanced Science and Technology in Experimental Mechanics, 2014, pp. 1–6.
[26] Designation: E8/E8M − 13a Standard Test Methods for Tension Testing of Metallic Materials 1.
[27] Dong Y.L., and Pan B., A Review of Speckle Pattern Fabrication and Assessment for Digital Image Correlation, Experimental Mechanics, Vol. 57, Issue 8, 2017, pp. 1161–1181.
[28] Reu P., All about Speckles: Contrast. Experimental Techniques, Vol. 39, Issue 1, 2015, pp. 1–2.
[29] Sciuti V.F., Canto R.B., Neggers J., and Hild F., On the Benefits of Correcting Brightness and Contrast in Global Digital Image Correlation: Monitoring Cracks during Curing and Drying of A Refractory Castable. Optics and Lasers in Engineering, Vol. 136, 2021, pp. 106316.
[30] Thai T.Q., Improvement of Ultraviolet Digital Image Correlation (UV-DIC) at Extreme Temperatures, Doctoral Dissertation, Utah State University, 2020.
[31] Jarrett S.R., The Effect of Bit Depth on High Temperature Digital Image Correlation Measurements, Doctoral Dissertation, Utah State University, 2021.
[32] Blaber J., Adair B., and Antoniou A., Ncorr: Open-Source 2D Digital Image Correlation Matlab Software. Experimental Mechanics, Vol. 55, Issue 6, 2015, pp. 1105–1122.
[33] Bigger R., Blaysat B., Boo C., Grewer M., Hu J., Jones A., Klein M., Raghavan K., Reu P., Schmidt T., Siebert T., Simenson M., Turner D., Vieira A., and Weikert T., A Good Practices Guidebook for Digital Image Correlation, International Digital Image Correlation Society, 2018, pp. 1–94.
[34] Shao X., and He X., Statistical error analysis of the inverse compositional gauss-newton algorithm in digital image correlation, Conference proceedings, In: Conference Proceedings of the Society for Experimental Mechanics Series. Springer Science and Business Media, LLC, 2017, pp. 75–76